Accepted Manuscript

Novel strategic approach for the thermo- and photo-oxidative stabilization of polyolefin/clay nanocomposites

Nadka Tzankova Dintcheva, Sahar Al-Malaika, Rossella Arrigo, Elisabetta Morici

PII: S0141-3910(17)30097-6

DOI: 10.1016/j.polymdegradstab.2017.04.014

Reference: PDST 8209

To appear in: *Polymer Degradation and Stability*

Received Date: 3 March 2017

Revised Date: 29 March 2017

Accepted Date: 11 April 2017

Please cite this article as: Dintcheva NT, Al-Malaika S, Arrigo R, Morici E, Novel strategic approach for the thermo- and photo-oxidative stabilization of polyolefin/clay nanocomposites, *Polymer Degradation and Stability* (2017), doi: 10.1016/j.polymdegradstab.2017.04.014.

Novel strategic approach for the thermo- and photo- oxidative stabilization of polyolefin/clay nanocomposites

Nadka Tzankova Dintcheva[*1,2], Sahar Al-Malaika[2], Rossella Arrigo[1], Elisabetta Morici[1]

[1]Dipartimento di Ingegneria Civile, Ambientale, Aerospaziale, dei Materiali, Università di Palermo, Viale delle Scienze, Ed. 6, 90128 Palermo, Italy

[2]Polymer Processing and Performance Research Unit, School of Engineering and Applied Science, Aston University, Aston Triangle, Birmingham, B4 7ET, UK

Abstract

Polyolefin/clay nanocomposites were prepared by melt mixing and their oxidative stability was studied under long-term thermo- and photo-oxidative test conditions in the absence and presence of a modified organo montmorillonite clay (OM-MMt) containing a chemically-bound hindered phenol antioxidant function, (AO)OM-Mt. It was found that nanocomposites based on both polyethylene (PE) and polyethylene-grafted-maleic anhydride (PEgMA) containing the (AO)OM-Mt gave a higher oxidative stability, along with better clay dispersion, compared to analogous PE or PEgMA-based nanocomposites containing an added (free) conventional antioxidant with a similar hindered phenol function (using the commercial hindered phenol Irganox® 1076). These findings can be explained in terms of the ability of the organo-modifier containing the in-built antioxidant function to act locally at the interface between the clay silicate layers and the polymer macromolecules thus contributing to the improved stability of the polymer observed both during long-term thermal- and photo- oxidative treatments.

Keywords: Clay Polymer Nanocomposites (CPN); Polyolefins; Stabilised organo montmorillonite; Thermo- and Photo-oxidative stabilization; Hindered Phenols.

[*] Corresponding author. Tel: +39 091 23863704. Fax: +39 091 23860841. E-mail address: nadka.dintcheva@unipa.it (N.Tz. Dintcheva).

1. Introduction

Polyethylene (PE) is one of the most extensively used polymers due to its attractive properties, mainly low-cost, high chemical resistance, safety and good processability [1]. For specific applications, PE can be modified by grafting using different functional groups such as maleic anhydride or acrylic acid [2-3]. In recent years, increasing attention has been given to the development of polyolefin/clay nanocomposites to explore their potential in more demanding applications and as alternatives to high-performance macro- and micro- composites in several areas of applications, e.g. food packaging and agriculture [4-6]. Clays are cheap, readily available and, even at low clay content, their PE-based nanocomposites exhibit better dimensional stability, flame retardancy, mechanical properties and gas permeation barrier when compared to the neat matrices [7-9]. These property enhancements can be achieved in a well distributed and homogeneously dispersed clay platelets in the host polymer. To achieve this, the naturally occurring (pristine) clays are first modified, typically with quaternary ammonium salts, to obtain the so-called organo-clays [10-11].

It is now generally accepted that the presence of organo-clays affects both the processing and the long-term oxidative stability of the clay-polymer nanocomposites; they accelerate the degradation process irrespective of the type of polymer used [12-15]. It has been confirmed [16-18] too that the products of the degradation process are the same as those of the host polymer itself albeit form at a much faster rate. The amount of products formed were shown to increase with increasing the clay content [19]. The pro-oxidant effect of the nano-clay fillers in polyolefin nanocomposites, which occurs under both thermal aging and UV exposure, is widely documented for LDPE/organo-clay nanocomposites [20-21]. The lower stability of clay-polymer nanocomposites with respect to the neat matrix is principally related to: (a) the decomposition of the quaternary ammonium ion (via the Hofmann elimination reaction), the generation of catalytic active sites (accepting single electrons from donor molecules of matrix with low ionization potential), and the formation of new radical species [22-23]; (b) impurities of the clay, such as iron ions, which have a catalytic effect on the decomposition of hydroperoxides produced during the matrix degradation [24] and (c) the stabilisers adsorption on the clay surface leading to their inactivation [25].

To overcome the issues related to the low thermo- and photo-oxidative stability of clay-containing nanocomposites, antioxidants and light stabilisers are usually added to extend the nanocomposites lifetime. However, sustained efforts to developing new formulations and procedures for the

stabilisation of the clay-polymer nanocomposites have not produced the desired improvement. Apart from the aforementioned problems (a-c), another reason for the above shortcoming could also be attributed to the poor distribution of the stabilizer(s) into the polymer matrix, and their migration and volatilization behavior during processing and long-term in-service use [26-27]. Recently [28, 29], an innovative approach was successfully applied for the stabilization of biopolymer based clay-containing nanocomposites using a modified organo-clay containing an in-built stabilising function. The stability, both during melt processing and under long-term thermal-oxidative conditions, of polyamide 11- and polylactic acid- based nanocomposites has been significantly improved with respect to that of the nanocomposites containing commercial clay and free antioxidant molecules.

In this work, a novel approach to the stabilisation of polyolefin-clay nanocomposites is described. PE and PEgMA used as the polymer matrices were melt processed with an organo-modified clay-containing an in-built (chemically attached) hindered phenol antioxidant function ((AO)OM-MMt) to produce an in-situ stabilized nanocomposites. The state of the clay dispersion and the morphology of the nanocomposites was investigated by X-ray diffraction, scanning and transmission electron microscopy (SEM and TEM), rheological analysis and differential scanning calorimetry (DSC). The thermo- and photo- oxidative stability of the PE/(AO)OM-MMt and PEgMA/(AO)OM-MMt nanocomposites were assessed through the analysis of the evolution of oxidation products with time by infrared spectroscopy and was compared to that of the neat matrices as well as with similarly produced nanocomposites containing commercially modified clay but produced in the presence and absence of an added (free) equivalent amount of the commercial hindered phenol antioxidant Irganox® 1076.

2. Experimental

2.1. Materials

The polyolefin used is a Low-Density Polyethylene (LDPE), produced by Versalis Spa under the trade name "Riblene FC30", has a melt flow index of 0.27 g/10 min (190 °C, 2.16 kg). The compatibiliser, Polybond 3009 (Crompton), is a high density polyethylene-graft-maleic anhydride (PEgMA), melting point 127°C, has a melt flow index of 5 g/10 min (190 °C, 2.16 kg) and 0.8 – 1.2wt% MA (Addivant data sheet) .

The natural unmodified montmorillonite Cloisite®Na^+ (MMt) is an ex. Southern Clay Products (Texas, USA) with ionic exchange capacity 92.6 meq/100g, specific gravity 2.86 g/cm^3 and d_{001}=1.17nm (2θ = 7.5°). The commercial organically modified montmorillonite, Cloisite®30B (CL30B), (OM-MMt) is an ex Southern Clay Products (Texas, USA) with ionic exchange capacity 90 meq/100g, specific gravity 1.98 g/cm^3 and d_{001}=1.85 nm (2θ = 4.8°). The organic modifier intercalated between the platelets of the clay is a bis-(2-hydroxyethyl) methyl tallow alkyl ammonium cation.

The stabilised organo-clay used here (AO)OM-MMt), which contained an antioxidant chemically linked to the organic modifier, was produced following a two-step chemical synthetic protocol, according to procedures reported earlier [28-29]. Specifically, the first-step involved the preparation of the antioxidant-containing organic modifier, named here (AO)OM, and the second-step was used to produce the antioxidant-containing organically modified clay (AO)OM-MMt, see **Figure 1.** Briefly, to prepare the (AO)OM, a reactive hindered phenol antioxidant containing a carboxylic acid function, see **Figure 1** for structure, was chemically reacted onto a quaternary ammonium salt (2-hydroxyethyl)oleylmethylbisammonium chloride (trade name ETHOQUAD®O/12 PG, MW=370.64 g/mol and formula: $C_{23}H_{48}NO_2Cl$ from Akzo Nobel®). The quaternary ammonium salt which was used to prepare the (AO)OM was the same as that present in the commercial organically modified clay Cloisite®30B. As reported previously [28], the (AO)OM contains a mixture of mono- and di-substituted compounds having one and two AO molecules (i.e. the in-built Irganox acid, 3-(3,5-di-tert-butyl-4-hydroxyphenyl) propanoic acid (see the chemical structure reported in Figure 1), synthesised from the commercial hindered phenol Irganox® 1076, (Octadecyl-3-(3,5-di-tert-butyl-4-hydroxyphenyl)-propionate) at a ratio of approximately 2:3 ((AO)OM-1: (AO)OM-2). The (AO)OM-MMt was then obtained by a cation-exchange reaction of (AO)OM with the commercial natural unmodified clay (MMt), see **Figure 1.** The overall content

of AO in (AO)OM-MMt clay was estimated to be around 9.1 wt.% (from TGA analysis) and the interlayer distance of (AO)OM-MMt calculated as d_{001}=2.05 nm (2θ = 4.3°).

2.2. Preparation of polyolefin-based nanocomposites

Clay based nanocomposites were prepared by melt mixing using a co-rotating twin-screw conical extruder, MiniLab Micro Compounder model CTW5, at 180°C, for 5 minutes at 100 rpm. The different clays were added in the molten polymer after 2 min of mixing. The nominal composition of all the polyolefin-based nanocomposites produced with modified and unmodified clays was: polyolefin/clay at 95:5 wt% (based on the inorganic content of the clay), see **Table 1**. For comparison, PE-based nanocomposites (PE/OM-MMt/AO and PEgMA/OM-MMt/AO) containing an added conventional hindered phenol antioxidant (Irganox® 1076) were prepared. The amount (0.45 wt%) of added Irganox 1076 was equivalent to that of the clay-bound AO functionality in the (AO)OM-MMt. Nanocomposites thin films (thickness about 100 micron) have been prepared by compression molding, using a laboratory hydraulic Carver press at 180 °C, for 5 min, under a pressure of 1500 psi.

2.3. Characterization

The X-Ray Diffraction (XRD) analysis of PE, PEgMA and polyolefin-based nanocomposites was performed using an Empyrean Series 2 X-Ray Diffraction (PANalytical): the spectra of the film samples were recorded in the range 3-30 deg (step size =0.025, scanning rate = 60s/step) and Cu-Kα radiation at wavelength λ= 0.1542 nm. The interlayer distance, d, was determined according to the Bragg's formula: $n\lambda = 2\, d \sin\theta$ (1),

Where, n is the diffraction order, λ - wavelength, θ - incident angle.

Scanning (SEM) and transmission (TEM) electron microscopy were used to characterize the morphologies of both polymeric matrices and nanocomposites. SEM analysis of the liquid nitrogen radially fractured (gold sputtered) surfaces were carried out on a Philips (Netherlands) ESEM XL30 microscope. TEM images of microtomed specimens were obtained using a JEOL JEM-2100 microscope under accelerated voltage of 200kV; ultrathin films (thickness ~100 nm) were cut from specimens embedded in epoxy resin using a Leica Ultra-microtome EM-UC6.

Rotational rheometry was applied to assess the rheological characteristics of PE, PEgMA and their nanocomposites. ARES G2 (TA Instrument) plate-plate rotational rheometer was run at T = 180°C under a 5% strain deformation (chosen after performing amplitude sweeps to ensure that the

dynamic tests are carried out in the linear viscoelasticity region). The complex viscosity (η*) and the storage (G') and loss (G") moduli were recorded as a function of frequency in the range 0.1-100 rad/sec. Differential scanning calorimetry (DSC) was performed using a Perkin-Elmer DSC7 calorimeter. All experiments were run under dry N_2 with samples of about 10 mg in 40µl sealed aluminium pans. Four calorimetric scans (heating scan: 30-160 °C; cooling scan: 160-30°C) were performed for each sample at heating and cooling rate of 10°C/min.

Fourier Transform Infrared Spectrometer, FTIR (Spectrum One, Perkin Elmer), was used to record IR spectra (16 scans, resolution of 4 cm^{-1}). FTIR analysis was carried out on films of neat PE, PEgMA and their nanocomposites. Measurements were made on three separately prepared batches of samples.

2.4. Thermo- and photo- oxidation stability

Thermo-oxidation of thin polymer and nanocomposite films (about 100 µm) was carried out in a forced-air circulation oven at 95°C. Ultraviolet (UV) exposure tests were carried out in a QU-V chamber containing eight UV-B lamps (Q-lab Corp, USA). The exposure cycle conditions was 8 h of light at T= 55 °C followed by 4 h condensation at T = 35 °C. The progress of both thermo- and photo- degradation was followed by FTIR spectroscopy. Carbonyl Index (CI) was calculated as the ratio of the areas of the aggregate carbonyl absorption peak (taken between 1850 and1600 cm^{-1}) to that of a polymer reference peak (measured between 1979 and 2110 cm^{-1}).

3. Results and discussion

3.1. Morphological, rheological and calorimetric characterization of PE- and PEgMA- based nanocomposites

The x-ray diffraction patterns of the neat polymers (PE, PEgMA) and their corresponding clay-nanocomposites, are shown in **Figure 2.** As expected, PE/MMt and PEgMA/MMt show small diffraction peaks at about 2θ = 7.5° due to the presence of MMt stacks. The PE/OM-MMt and PE/OM-MMt/AO samples display diffraction peaks at about 2θ = 4.5° attributable to the presence of intercalated OM-MMt stacks. However, this peak appears to be very weak in the PEgMA-based nanocomposites (containing OM-MMt and OM-MMt/AO), **Figure 2 (b)**, which would suggest the prevalence of an exfoliated morphology. The small shoulder observed at 2θ around 6.0° may be due to collapsed MMt stacks [10]. In the case of PE/(AO)OM-MMt and PEgMA/(AO)OM-MMt, the characteristic clay peaks in the XRD patterns, were not detectable which could suggest a preponderance of an exfoliated clay morphology procured through an intrinsically large steric hindrance of the (AO)OM moiety.

The state of clay dispersion in the PE and PEgMA based nanocomposites was further assessed by SEM. Close examination of the micrographs (**Figure 3**) indicates the presence of large silicate particles (about 2μm) associated with a poor state of dispersion of the unmodified clay in the MMt-containing samples. A more homogenous dispersion was observed in PE and PEgMA nanocomposites containing OM-MMt, and no clay aggregates were apparent in the micrographs of the nanocomposites containing (AO)OM-MMt. the improved dispersion is probably due to the greater interlayer distances between the platelets in these samples which helps in helping the intercalation of the polymer network within the silicate layers which is in agreement with the XDR results. The exfoliated morphology in both PE- and PEgMA nanocomposites containing (AO)OM-MMt was further confirmed by TEM (see **Figure 4**) analysis.

Moreover, the state of nanofiller dispersion in the polymer-based nanocomposites was also examined by rheological measurements [12]. Viscosity, and storage (G') and loss (G'') moduli were determined and their dependency on frequency was followed. These measurements show that the addition of clay has only a negligible effect on the rheological behaviour of PE-based nanocomposites, see **Figure 5 (a-b)**. Indeed, the values of the rheological functions of PE-based nanocomposites were very similar to those of the neat matrix. As to the PEgMA-based nanocomposites, the addition of nanoclays brought about an increase of the viscosity and moduli

values, see **Figure 5 (c-d)**, indicating that the functionalization of PE with MA functionalities has a beneficial effect on the state of dispersion of the nanoclay.

Differential scanning calorimetric analysis, see **Figure 6 and Table 2**, indicates that the different clays do not impart any nucleating effect since the melting temperatures and enthalpies (enthalpy values corrected for the clay content based on second heating scan) of all the PE- and PEgMA based nanocomposites were almost similar to those of the neat matrices.

3.2. Long-term thermo-oxidative stability of PE- and PEgMA- based nanocomposites

To verify the effectiveness of the proposed method for the stabilization of polyethylene-clay nanocomposites, thin films of PE- and PEgMA- based nanocomposites have been subjected to thermo-oxidative aging in an air circulating oven at 95^{o}C and the progress of the degradation phenomena was monitored by FTIR analysis. In **Figure 7 (a-c),** the collected spectra for different PE-based nanocomposite samples as a function of the thermo-oxidation time are reported. It is well known [21] that the thermo-oxidation mechanism of PE proceeds through the formation of oxygen containing groups. Their accumulation is reflected in the growth of an extensive carbonyl absorption peak in the FTIR spectra in the range 1850-1600 cm^{-1}. Specifically, the main products of the PE degradation (**Figure 7)** are the carboxylic acids (1710 cm^{-1}) and ketones (1713 cm^{-1}), esters (1730 cm^{-1}) and γ-lactones (1780 cm^{-1}). Further examination of the different samples confirms also the earlier literature findings [21, 24] that the presence of the OM-MMt nano-clay exacerbates the PE degradation process. However, the PE/(AO)OM-MMt test sample examined here did not show a distinguishable oxidation signatures in its IR spectrum even after 500 h of thermo-oxidative ageing (**see Figure 7 (c)**), which would suggest that, under these conditions, the AO-containing clay is able to stabilise the PE matrix against the thermo-oxidative degradation. To qualitatively evaluate the progress of the oxidative degradation in the clay-polymer samples, the carbonyl index was plotted, **see Figure 7 (d),** as a function of the thermo-oxidation time. As inferred from the analysis of the FTIR spectra, the presence of both commercial clays (MMt and OM-MMt) leads to a more rapid accumulation of oxidative (carbonyl-based) degradation products with respect to the neat PE. The PE-nanocomposite containing the clay-bound hindered phenol antioxidant ((AO)OM-MMt), on the other hand, shows a significant reduction in the rate of thermo-oxidation of the nanocomposite; this is similar to, or possibly slightly better than, when free molecules of a commercial hindered phenol (Irganox 1076) are added to the formulation.

The thermo-oxidative behaviour of the PEgMA-based nanocomposites was similarly evaluated by subjecting thin films to thermo-oxidative ageing and following the evolution of the oxidation profile

by IR with ageing time, see **Figure 8 (a-b)** for neat PEgMA and PEgMA/(AO)OM-MMt. It can be seen that only slight changes were observed after about 500h of ageing. It is well known [30] that thermo-oxidative degradation of PEgMA proceeds with the formation of oxygen-containing groups and the hydroxyl groups formed as a consequence of thermal oxidation are able to react further with the MA functionalities to form crosslinked structures, hence the accumulation of oxygen-containing groups is not easily detectable by FTIR analysis. If crosslinked structures are formed, then an increase in the molecular weight and viscosity of the polymer can be expected to occur at the same time. To examine this possibility, rheological analysis of these nanocomposites was conducted. Viscosity plots of PEgMA-nanocomposite samples subjected to 500h thermo-oxidative ageing and the corresponding normalized viscosity values (i.e. viscosity after ageing , η_t, over the corresponding unaged values,$\eta_{0;}$ η_t/η_0) are shown in **Figure 8 (c and d)**. It is clear that the normalized viscosity values for PEgMA and PEgMA nanocomposites containing MMt and OM-MMt are much higher than 1 indicating an increase in their viscosity, and implicitly their molecular weight, during thermo-oxidation thus supporting the formation of some polymer crosslinking structures. Addition of the conventional antioxidant Irganox 1076 resulted in lower normalized viscosity values highlighting the beneficial effect of adding the antioxidant. However, for nanocomposite containing the clay-grafted antioxidant ((AO)OM-MMt), even lower values of their normalized viscosity can be seen (values closer to 1) indicating that the extent of change in the viscosity and molecular weight, as consequence of thermo-oxidative ageing, is lower in the presence of the in-built antioxidant compared to that of the added AO. This suggests that a lower extent of crosslinking, which occurs as a direct consequence of thermal oxidation, takes place in the presence of a clay-grafted antioxidant, compared to that of a conventionally added AO, which is most likely to be due to the higher stabilising efficacy of the former.

Overall, the stabilising performance of the OM-immobilised-AO can be attributed to a number of factors: (i) the anchoring of AO functionalities would avoid the typical migration and volatilization issues associated with freely mobile AO molecules, (ii) the gathering of the AO functionalities at the interface region between the inorganic clay and the matrix (in an exfoliated morphology) makes the AO groups more readily available in the most critical area for the onset of degradation.

3.3. Photo-oxidation stability of PE- and PEgMA- based nanocomposites

To investigate the possible beneficial effect of the clay-immobilized AO on the long-term photo-oxidative stability of the nanocomposites, thin films of all the samples were subjected to UVB exposure and the progress of their photo-degradation was monitored by FTIR analysis. The spectra

of PE- and PEgMA- based nanocomposites as a function of the photo-exposure time are shown in **Figures 9 (a-c) and 10 (a-c),** respectively, along with the calculated values of the carbonyl indices (Figures 9 (d) and 10 (d)). The addition of OM-MMt to PE leads to a significant increase in the photo-oxidation rate, due to the presence of iron ion impurities in the silicates and to the formation of acidic sites on the silicate layers and α-olefins resulting from the Hoffman elimination reaction of the OM during the processing of the nanocomposites [21, 24]. **Figure 9 (d)** shows also that in the presence of the added (free) AO (Irganox 1076), the photo-oxidation rate of the nanocomposite sample (PE/OM-MMt/AO) is significantly reduced. The ability of the added AO (Irganox 1076) to effectively scavenge the free radicals initially formed during the melt processing step, along with its weak UV stabilizing action, would be responsible for the the observed improvement in the nanocomposite photo-oxidative stability compared to when no antioxidant is present. However, it is also very clear from this figure, that the **tying-in** of AO molecules on the OM in the clay has given rise to an even more effective level of stabilization reflected in a slower photo-oxidation rate of the nanocomposite containing the AO-in-situ modified clay (PE/(AO)OM-MMt); the rate of photo-oxidation (from the build-up of carbonyl-containing oxidation products) of the nanocomposite containing clay-grafted AO is slightly slower than that of PE especially at higher exposure times. This excellent stabilizing effect is a consequence of the availability of the free radical scavenging-clay-grafted AO where it is needed most at the interface between the inorganic silicate layers and the polymer network.

In the case of PEgMA and its nanocomposites, the rate of degradation of these samples upon UVB exposure is affected by the photolytic instability of the MA functionality (**Figure 10 (d)** shows that PE-gMA photoxidises at a faster rate than PE). The presence of MMt does not significantly affect the rate of photo-oxidation of PEgMA, probably because the photolytic instability of the MA functionalities pre-determines the stability of the PEgMA/MMt under such photoxidative conditions. However, the presence of the organically modified clay (OM-MMt) can be seen to drastically increase the rate of the nanocomposite photo-oxidation, and this has been suggested in the literature [21] to be due to unfavorable interactions that occur, in this case under the UVB-exposure conditions, between the MA functionalities, the clay and the alkyl ammonium surfactant and its decomposition products. Addition of the conventional AO, Irganox 1076, slows down, but only slightly, the rate of photo-oxidation of PEgMA/OM-MMt nanocomposite due to their protection action against the radical formation during the processing step. In contrast, the in-built AO molecules within the clay structure is clearly seen (**Figure 10 (d))** to gives rise to a more substantial reduction in the rate of photo-oxidation of the PEgMA/OM-MMt nanocomposite

sample. This must be due to a further improved ability of the clay-grafted AO molecules to trap more radicals during processing for all the reasons highlighted above.

4. Conclusions

For a successful large-scale application of polyolefin-based clay-containing nanocomposites, the control of their long-term thermo- and photo- oxidative stability is a crucial point. In this work, PE- and PEgMA- based nanocomposites having a newly modified organo-clay containing chemically bound hindered phenol antioxidant molecules ((AO)OM-MMt) have been prepared by melt mixing and their long-term thermo- and photo- oxidative stability has been compared with that of nanocomposites containing OM-MMt and a free (added) commercial antioxidant having the same AO-functionality (Irganox 1076). The results highlight the beneficial effect that the clay-in-built antioxidant (AO)OM-MMt affords to the melt processed clay-nanocomposites with respect to enhancing both their overall thermal and photoxidative stability. The anchoring of the antioxidant molecules on the clay (in (AO)OM-MMt) eliminates the possibility of their physical loses and increases their availability at the interface between the silicates and the macromolecules. This, along with the very good intercalated/exfoliated clay morphology they impart to the nanocomposite systems, makes this approach a highly suitable route for the stabilization of polyolefin-based clay-containing nanocomposites.

Acknowledgments: This work has been financially supported by EU in the field of Marie Curie Action–PEOPLE 2011–IEF, (N:300302), Project: NANOSTAB-GB - Novel Nano-Stabilisation for Green Bioplastic Nanocomposites.

References

[1] D. Feldman, Polyolefin, olefin copolymers and polyolefin polyblend nanocomposites, J. Macromol. Sci. Pure 53 (2016) 651-658.

[2] K.H. Wang, M.H. Choi, C.M. Koo, Y.S. Choi, I.J. Chung, Synthesis and characterization of maleated polyethylene/clay nanocomposites, Polymer 42 (2001) 9819-9826.

[3] N. Tz. Dintcheva, E. Morici, R. Arrigo, F. P. La Mantia, Interaction in POSS-poly(ethylene-co-acrylic acid) nanocomposites Polym. J. 46 (2014) 160-166.

[4] M.T. Ton-That, F. Perrin-Sarazin, K.C. Cole, M.N. Bureau, J. Denault, Polyolefin nanocomposites: Formulation and development, Polym. Eng. Sci. 44 (2004) 1212-1219.

[5] N.Tz. Dintcheva, G. Filippone, F.P. La Mantia, D. Acierno, Photo-oxidation behaviour of polyethylene/polyamide 6 blends filled with organomodified clay: Improvement of the photo-resistance through morphology modification, Polym. Degrad. Stab. 95 (2010) 527-535

[6] M. Alexandre, P. Dubois, Polymer-layered silicate nanocomposites: preparation, properties and uses of a new class of materials, Mat. Sci. Eng. R 28 (2000) 1–63.

[7] S. Sinha Ray, M. Okamoto, Polymer/layered silicate nanocomposites: A review from preparation to processing, Progr. Polym. Sci. 28 (2003) 1539-1641.

[8] S. Pavlidou, C.D. Papaspyrides, A review on polymer-layered silicate nanocomposites, Progr. Polym. Sci. 33 (2008) 1119-1198.

[9] B. Tan, N.L. Thomas, A review of the water barrier properties of polymer/clay and polymer/graphene nanocomposites, J. Membrane Sci. 514 (2016) 595-612.

[10] S. Filippi, M. Paci, G. Polacco, N.Tz. Dintcheva, P. Magagnini, On the interlayer spacing collapse of Cloisite® 30B organoclay, Polym. Degrad. Stab. 96 (2011) 823-832.

[11] S. Hotta, D.R. Paul, Nanocomposites formed from linear low density polyethylene and organoclays, Polymer 45 (2004) 7639–7654.

[12] L. Botta, N.Tz. Dintcheva, F.P. La Mantia, The role of organoclay and matrix type in photo-oxidation of polyolefin/clay nanocomposite films Polymer Degradation and Stability 94 (2009) 712-718.

[13] H. Qin, C. Zhao, S. Zhang, G. Chen, M. Yang, Photooxidative degradation of polyethylene/montmorillonite nanocomposite. Polym. Degrad. Stab. 81 (2003) 497-500.

[14] H. Qin, S. Zhang, H. Liu, S. Xie, M. Yang, D. Shen, Photo-oxidative degradation of polypropylene/montmorillonite nanocomposites Polymer 46 (2005) 3149-3156.

[15] B. Mailhot, S. Morlat, J.L. Gardette, S. Boucard, J. Duchet, J.F. Gérard, Photodegradation of polypropylene nanocomposites, Polym. Degrad. Stab. 82 (2003) 163–167.

[16] G. Gutiérrez, A. Fayolle, G. Régnier, J. Medina, Thermal oxidation of clay-nanoreinforced polypropylene, Polym. Degrad. Stab. 95 (2010) 1708–1715.

[17] S. Morlat, B. Mailhot, D. Gonzalez, J.L. Gardette, Photo-oxidation of polypropylene /montmorillonite nanocomposites. 1. Influence of nanoclay and compatibilizing agent, Chem. Mater. 16 (2004) 377-83.

[18] A.P. Kumar, D. Depan, N.S. Tomer, R.P. Singh, Nanoscale particles for polymer degradation and stabilization-Trends and future perspectives, Progr. Polym. Sci. 34 (2009) 479-515.

[19] R. Scaffaro, L. Botta, M. Ceraulo, F.P. La Mantia, Effect of kind and content of organo-modified clay on properties of PET nanocomposites, J. Appl. Polym. Sci. 122 (2011) 384-392.

[20] Q. Huaili, Z. Chungui, Z. Shimin, C. Guangming, Y. Mingshu, Photo-oxidative degradation of polyethylene/montmorillonite nanocomposite, Polym. Degrad. Stab. 81 (2003) 497-500.

[21] N.Tz. Dintcheva, S. Al-Malaika, F.P. La Mantia, Effect of extrusion and photo-oxidation on polyethylene/clay nanocomposites, Polym. Degrad. Stab. 94 (2009) 1571-1588.

[22] R.K. Shah, D.R. Paul, Organoclay degradation in melt processed polyethylene nanocomposites, Polymer 47 (2006) 4075-4084.

[23] W. Xie, Z. Gao, W.-P. Pan, D. Hunter, A. Singh, R. Vaia, Thermal Degradation Chemistry of Alkyl Quaternary Ammonium Montmorillonite, Chem. Mater. 13 (2001) 2979-2990.

[24] F.P. La Mantia, N.Tz. Dintcheva, V. Malatesta, F. Pagani, Improvement of photo-stability of LLDPE-based nanocomposites, polym. Degrad. Stab. 91 (2006) 3208-3213.

[25] S. Morlat-Therias, B. Mailhot, J.L. Gardette, C. DaSilva, B. Haidar, A. Vidal, Photooxidation of ethylene-propylene-diene/montmorillonite nanocomposites. Polym. Degrad. Stab. 2005, 90, 78-85.

[26] B. Mailhot, S. Morlat, J.L. Gardette, S. Boucard, J. Duchet, J.F. Gerard, Photodegradation of polypropylene nanocomposites Polym. Degrad. Stab. 82 (2003) 163-167.

[27] Al-Malaika S., Ed. In Reactive Modifiers for Polymers; Blackie Academic & Professional, London, 1997.

[28] N.Tz. Dintcheva, S. Al-Malaika, E. Morici, Novel organo-modifier for thermally-stable polymer-layered silicate nanocomposites, Polym. Degrad. Stab.,122 (2015) 88–101.

[29] N.Tz. Dintcheva, S. Al-Malaika, E. Morici, R. Arrigo, Thermo-oxidative stabilization of polylactic acid-based nanocomposites through the incorporation of clay with in-built antioxidant activity, J. Appl. Polym. Sci. in press, DOI: 10.1002/app.44974

[30] J-W. Huang, W-ch. Lu, M-Y Yeh, Ch-Hs Lin, I-Sh. Tsai, Unusual thermal degradation of maleic anhydride grafted polyethelene, Polym. Eng. Sci., 48 (2008) 1550-1554.

Caption for Tables and Figures

	Polymer, wt.%	MMt, wt.%	OM-MMt, wt.%	AO, wt.%	(AO)OM-MMt, wt.%
PE	100	---	---	---	---
PE/MMt	95	5	---	---	---
PE/OM-MMt	95	---	5	---	---
PE/OM-MMt/AO	94.55	---	5	0.45	---
PE/(AO)OM-MMt	95	---	---	---	5
PEgMA	100	---	---	---	---
PEgMA/MMt	95	5	---	---	---
PEgMA/OM-MMt	95	---	5	---	---
PEgMA/OM-MMt/AO	94.55	---	5	0.45	---
PEgMA/(AO)OM-MMt	95	---	---	---	5

Table 1. Composition of formulated PE and PEgMA -based systems

	PE-based		PEgMA-based		
	T_m, °C	ΔH_m, J/g	T_{m1}, °C	T_{m2}, °C	ΔH_m, J/g
---	106.3	73.4	117.2	119.6	73.5
MMt	105.8	73.8	117.3	119.8	74.2
OM-MMt	106.4	72.2	118.4	120.5	70.7
OM-MMt/AO	106.2	76.5	118.0	120.1	71.8
(AO)OM-MMt	106.8	71.7	118.8	120.2	70.4

Table 2. Melting temperature (Tm) and melting enthalpy (ΔHm), relatively to the second heating scan from DSC analysis, for neat matrices and all the investigated nanocomposites

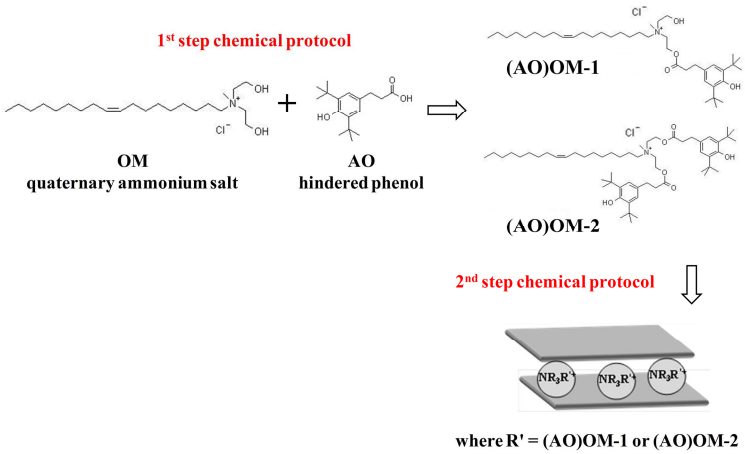

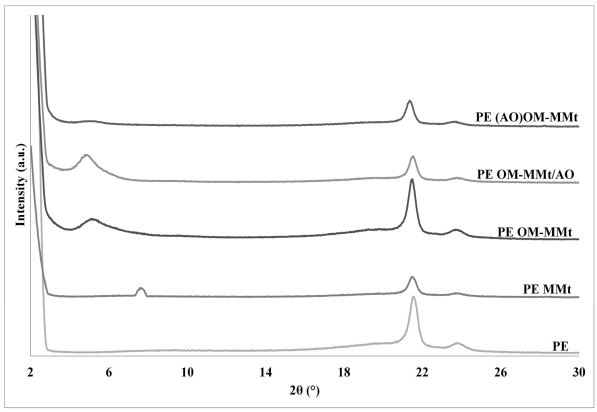

(a)

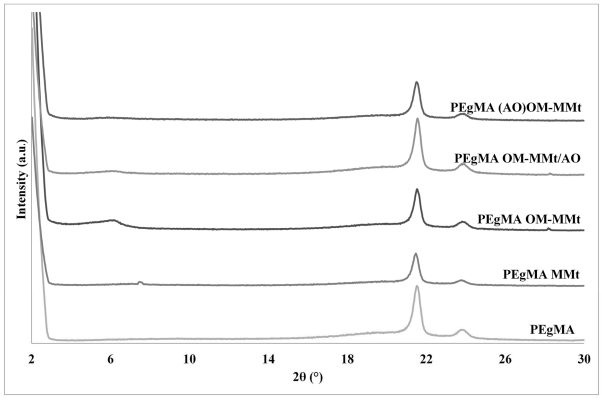

(b)

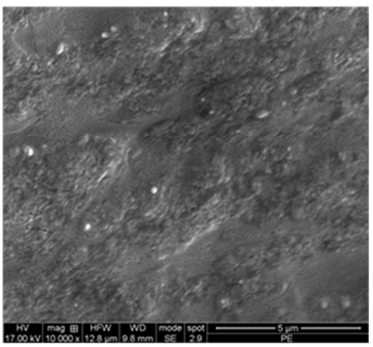

PE

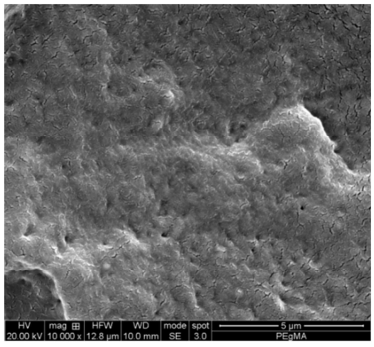

PEgMA

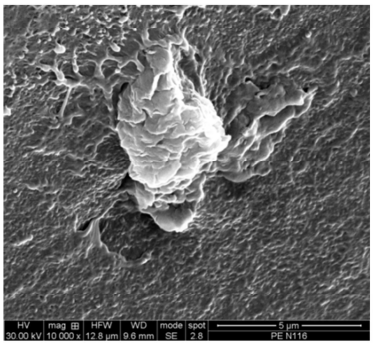

PE/MMt

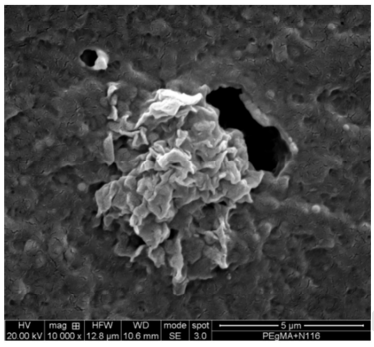

PEgMA/MMt

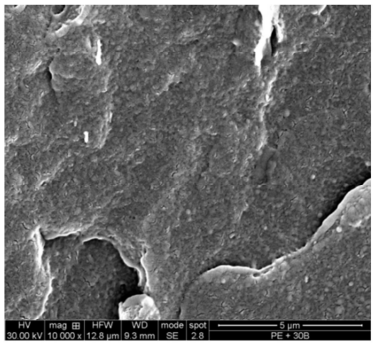

PE/OM-MMt

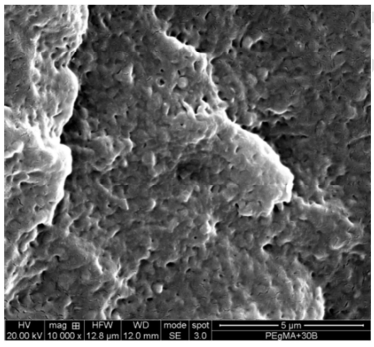

PEgMA/OM-MMt

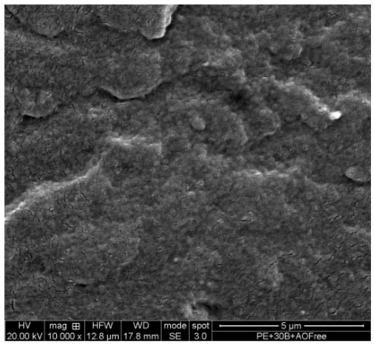

PE/OM-MMt/AO

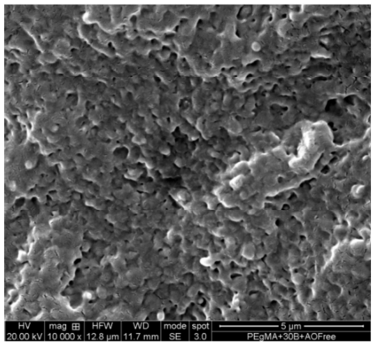

PE/OM-MMt/AO

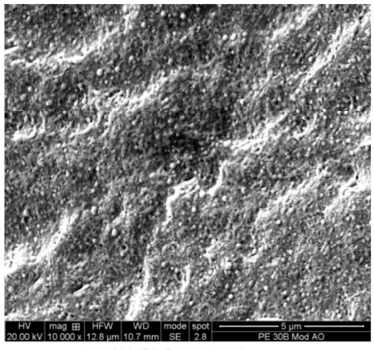

PE/(AO)OM-MMt

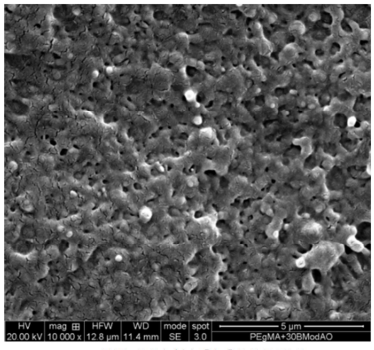

PEgMA/(AO)OM-MMt

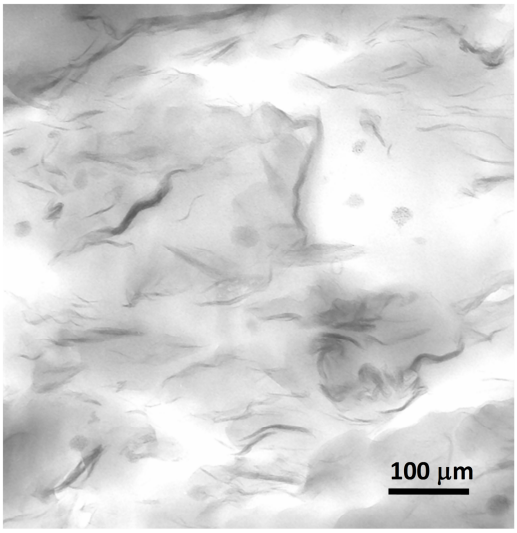

PE/(AO)OM-MMt

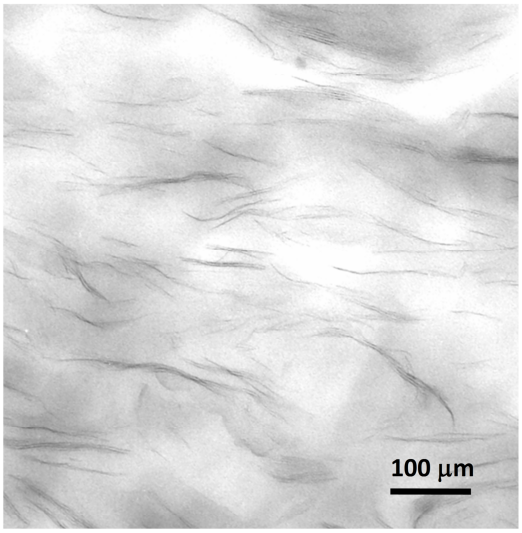

PEgMA/(AO)OM-MMt

PE-based nanocomposites

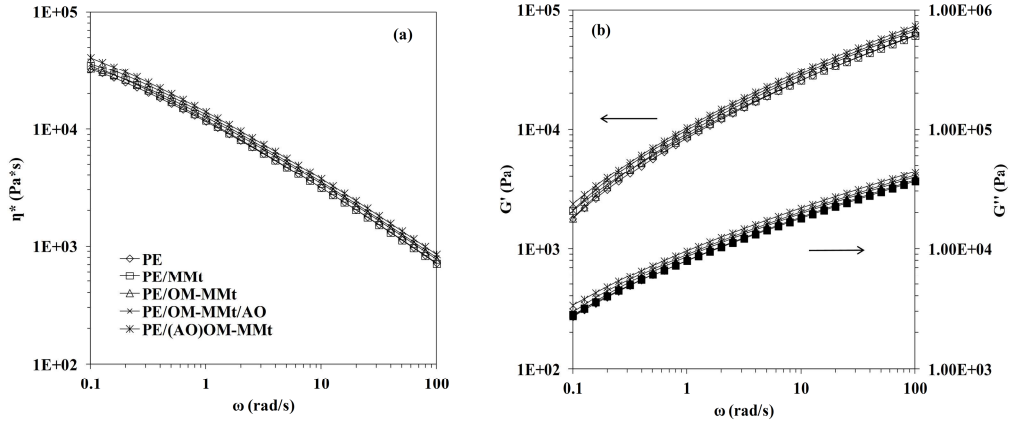

PEgMA-based nanocomposites

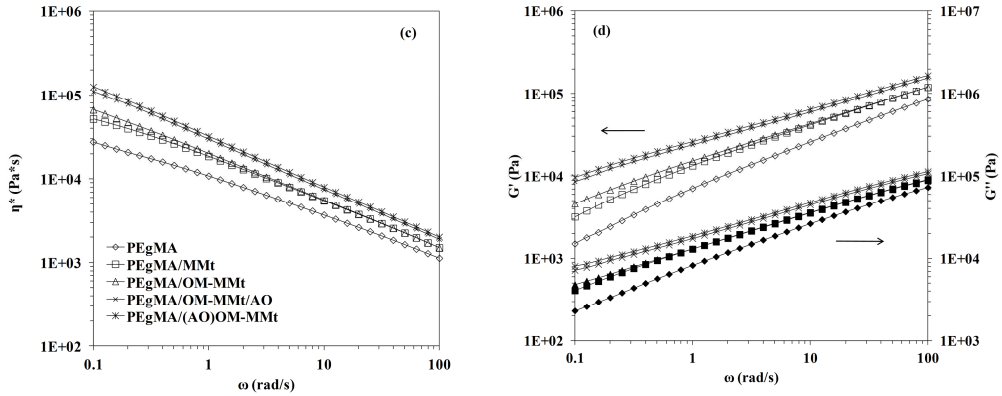

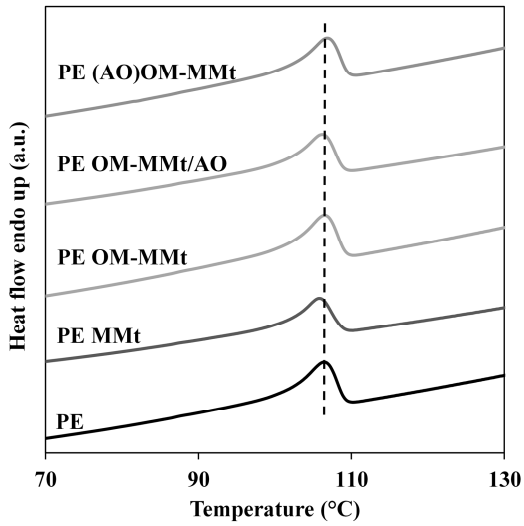

(a)

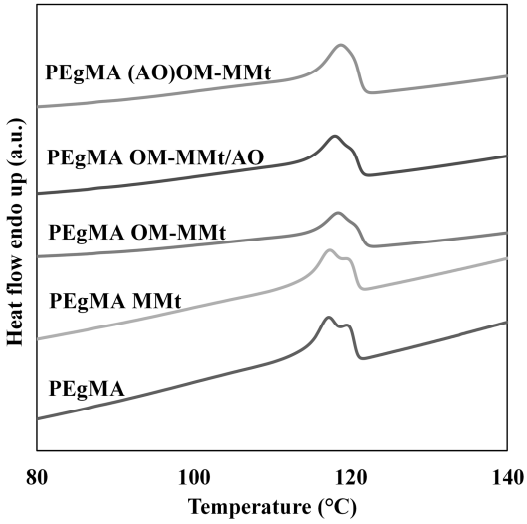

(b)

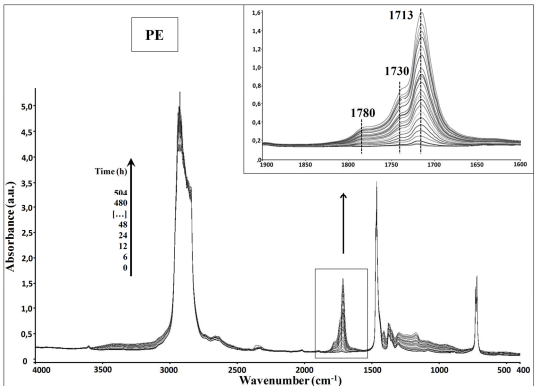

(a)

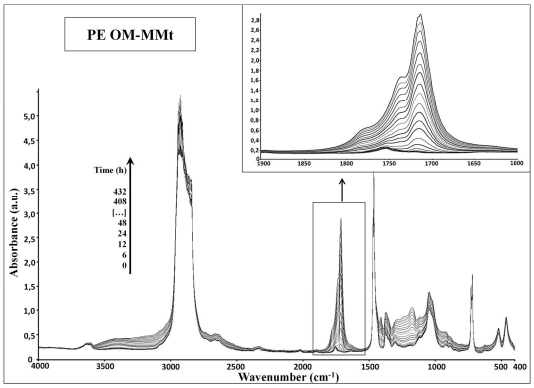

(b)

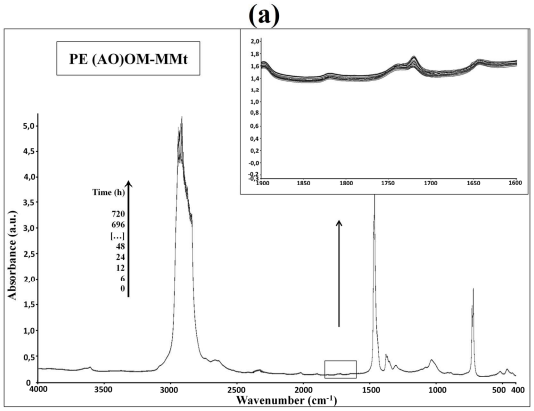

(c)

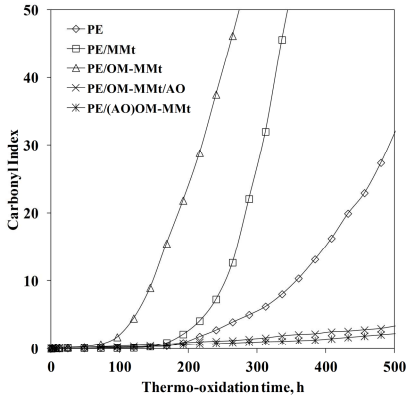

(d)

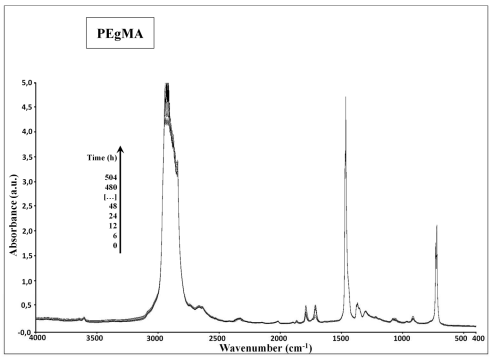

(a)

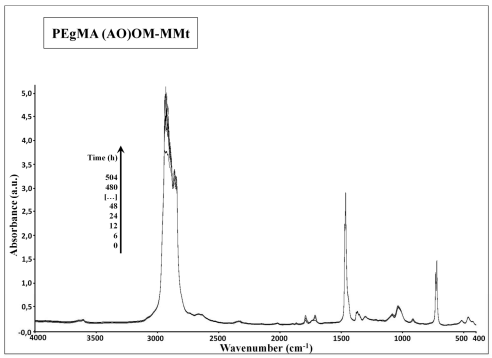

(b)

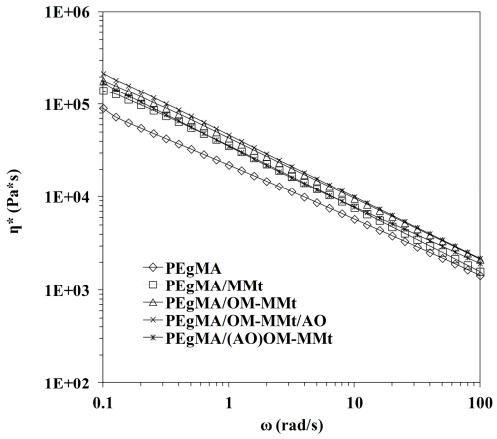

(c)

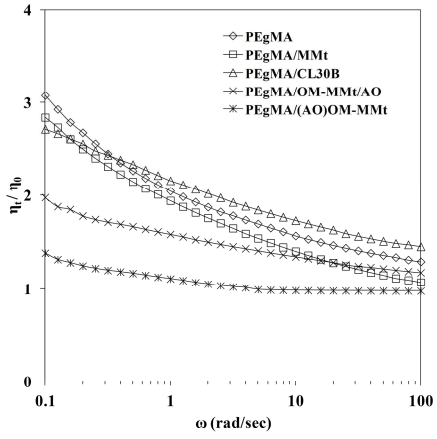

(d)

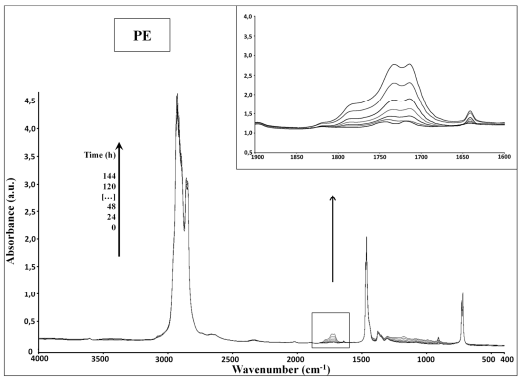

(a)

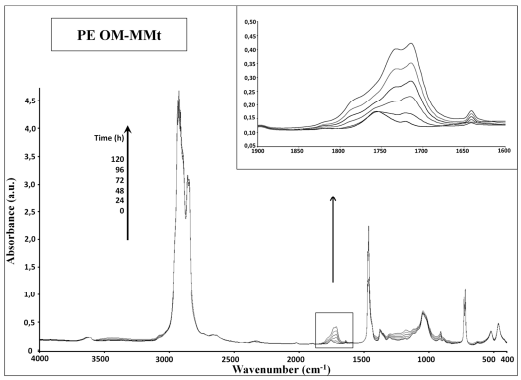

(b)

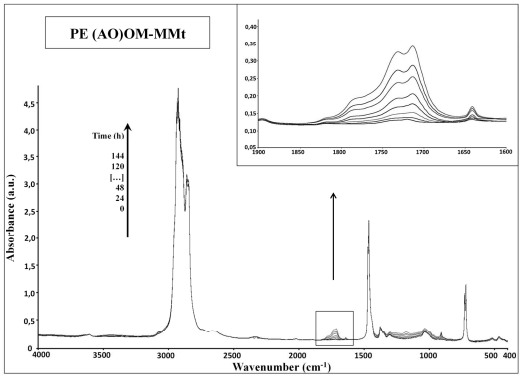

(c)

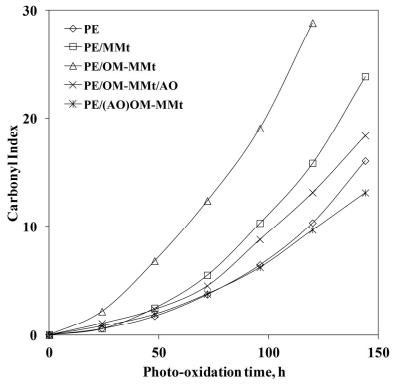

(d)

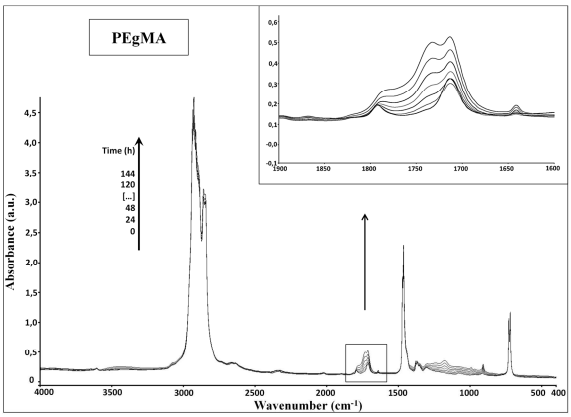

(a)

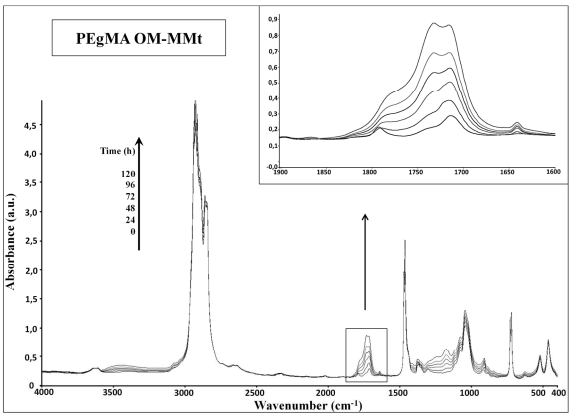

(b)

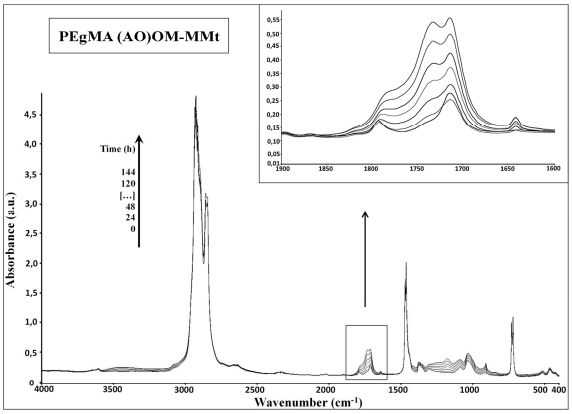

(c)

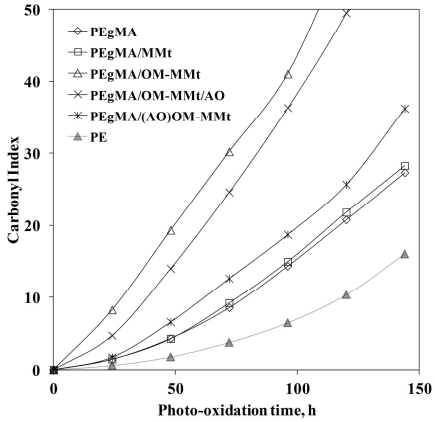

(d)